PHYSICAL REVIEW A

STATISTICAL PHYSICS, PLASMAS, FLUIDS, AND RELATED INTERDISCIPLINARY TOPICS

THIRD SERIES, VOLUME 42, NUMBER 6 15 SEPTEMBER 1990

Escape-time distributions of a periodically modulated bistable system with noise

Ting Zhou and Frank Moss
Department of Physics, University of Missouri at St. Louis, St. Louis, Missouri 63121

Peter Jung
Institute of Physics, University of Augsburg, Memminger Strasse 6, D-8900 Augsburg, Federal Republic of Germany
(Received 24 April 1990)

In this paper a periodically driven, bistable system with additive noise is considered in the overdamped limit. Here we have adopted the probability density of residence times as the tool for dynamical studies on the system. We contrast this to the body of previous work, in the area now known as "stochastic resonance," wherein the power spectral density was the preferred physical quantity. It is shown, both by analytic theory and by analog simulations, that the density of residence times has a detailed structure reflective of the inherent symmetries of the system. Closed-form expressions are developed for the distribution function as well as for several averaged quantities of interest. It is emphasized that all our analytic results predict observable physical quantities, which are then demonstrated with measurements on the analog simulator.

I. INTRODUCTION

There is a great deal of interest in modulated multistable systems, which are representative of a variety of physical systems, ranging from modulated Josephson-junction systems,[1,2] the diffusion of particles in periodic potentials under the influence of harmonic noise,[3] superionic conductors,[4] and excited chicken hearts[5] to the dithered ring laser[6] and other laser systems.[7] In many of these systems noise of high dimension is either an inherent problem that must be dealt with[8] or the primary focus of attention.[9] An example of a system wherein the noise is crucial to the dynamical behavior is illustrated by the observation of stochastic resonance in a ring laser,[10] an experiment that has refocused attention on modulated noisy systems. In a field that began with early attempts to understand the periodic recurrences of the Earth's ice ages[11,12] and continued with an electronic-circuit realization,[13] this recent experiment has stimulated a new body of theory[9,14–17] as well as analog simulations.[18,19] In the large majority of the works cited, and in particular since the experimental demonstration of the existence of a maximum in the signal-to-noise ratio, the focus of attention was on the power spectral density of the noisy modulated system. As an archetype of such systems with inertia, the power spectrum of the modulated Duffing oscillator with noise has been of historical[20] and continuing[17,18,21] interest. In the context of noise-induced chaos and eigenvalue statistics, periodically driven stochastic systems have been studied very recently.[22]

Here, in contrast, we present the results of a theory and an analog simulation wherein the probability density of residence times is the object of interest. In certain applications—for example, when a single escape from a local potential minimum or from an unstable state is the event of interest—this quantity reveals the dynamics more transparently than the power spectrum. A residence-time probability theory has already been presented for a modulated system of discrete random walkers on the interval,[23] and the results of early analog simulations were obtained for the decay of unstable states.[24] In the case of stochastic resonance, high-precision measurements of this quantity were first presented in Ref. 19(b). The analog simulation is a straightforward adaptation of techniques already reviewed.[19] The background and development of interest in modulated, noisy systems has been previously elaborated in more detail[9,19] and will not be further discussed here.

This paper is organized as follows. In Sec. II, we present the theoretical development and the closed-form results for the residence distribution and for certain averages of interest. Then in Sec. III we examine certain asymptotic limits of the theory that yield results in closed form. In Sec. IV we present the results of the analog simulation and compare them to the theory. We present some further results of the simulation that have not yet been considered by the theory, and we finally display the

now familiar "resonance" curve *but here based on properties of the residence-time probabilities,* rather than on the more usual power spectra. Finally, in Sec. V we summarize our results and present some further discussion.

II. THEORY

In this section a theoretical approach to the residence-time distribution is developed in the limiting case of small modulation frequencies. The theory is based on the adiabatic approach for the escape rate out of a potential well developed recently in Ref. 16(a). Our starting point is the Langevin equation:

$$\begin{aligned}&\dot{x}=x-x^3+A\sin(\omega_0 t+\phi)+\sqrt{D}\,\xi(t)\ ,\\&\langle\xi(t)\rangle=0\ ,\\&\langle\xi(t)\xi(t')\rangle=2\delta(t-t')\ ,\end{aligned}\tag{1}$$

where D is the noise strength.[25,26] The system variable x is dimensionless as in the simulation, and we take the modulation strength A to be positive without loss of generality. For small frequencies, that is, for $\omega_0 \ll \exp(-1/4D)$, the probability distribution for x reads[16(a)]

$$P_{\rm ad}(x,t)=\frac{1}{Z_0}\frac{\exp[-x^4/4D+x^2/2D+(Ax/D)\sin(\omega_0 t+\phi)]}{\sum_{n=0}^{\infty}\frac{1}{n!}\left[\frac{A^2\sin^2(\omega_0 t+\phi)\sqrt{2D}}{D^2}\right]^n D_{-n-\frac{1}{2}}(-1/\sqrt{2D})}\ ,\tag{2}$$

where $Z_0=\exp(1/8D)(2D)^{1/4}\sqrt{\pi}$ and $D_n(x)$ denote parabolic cylinder functions.[27] The time-dependent escape rates[28] out of the right well (r^-) and out of the left well (r^+) are estimated for small noise strength D by the Kramer's formula,

$$r^{\mp}(\omega_0 t+\phi)=\frac{1}{\pi}(|V''_{\rm ad}(x_u,t)|V''_{\rm ad}(x_s^{\pm},t))^{1/2}\times\exp\left[-\frac{\Delta V^{\pm}_{\rm ad}(t)}{D}\right]\ ,\tag{3}$$

where the adiabatic potential $V_{\rm ad}(x,t)$ is given by

$$\begin{aligned}V_{\rm ad}(x,t)&=x^4/4-x^2/2-Ax\sin(\omega_0 t+\phi)\\&\quad+D\ln\sum_{n=0}^{\infty}\frac{1}{n!}\left[\frac{A^2\sin^2(\omega_0 t+\phi)\sqrt{2D}}{D^2}\right]\times D_{-n-1/2}(-1/\sqrt{2D})\ .\end{aligned}\tag{4}$$

In Eq. (3) the $x_s^{\pm}$ are the time-dependent locations of the right (+) and left (−) minima of the adiabatic potential $V_{\rm ad}(x)$, and x_u denotes the position of the maximum (unstable state) between them. The time-dependent barrier heights are denoted $\Delta V^{\pm}_{\rm ad}(t)$. The last term in Eq. (4) is not x dependent and thus does not enter into the calculations for $x_s^{\pm}$ and x_u. To second order in the modulation strength A, we find

$$\begin{aligned}&x_u=-A\sin(\omega_0 t+\phi)+O(A^3)\ ,\\&x_s^{\pm}=\pm1+(A/2)\sin(\omega_0 t+\phi)\\&\qquad\mp\tfrac{3}{8}A^2\sin^2(\omega_0 t+\phi)+O(A^3)\ ,\end{aligned}\tag{5a}$$

which results in the barrier height

$$\begin{aligned}\Delta V^{\pm}_{\rm ad}&=\tfrac{1}{4}\pm A\sin(\omega_0 t+\phi)\\&\quad+\tfrac{3}{4}A^2\sin^2(\omega_0 t+\phi)+O(A^3)\ .\end{aligned}\tag{5b}$$

Inserting Eqs. (5a) and (5b) into Eq. (3), we find for the time-dependent escape rates to second order in A, following Ref. 16(a),

$$\begin{aligned}r^{\pm}(\omega_0 t+\phi)&=r_0[1\mp\tfrac{3}{4}A\sin(\omega_0 t+\phi)\\&\quad-\tfrac{69}{32}A^2\sin^2(\omega_0 t+\phi)]\\&\quad\times\exp[\pm(A/D)\sin(\omega_0 t+\phi)\\&\quad-(3A^2/4D)\sin^2(\omega_0 t+\phi)]\ ,\end{aligned}\tag{6a}$$

valid for

$$\tfrac{1}{4}\gg D\gg 1/[4|\ln(\omega_0/\sqrt{2})|]\ ,$$

where r_0 is the Kramer's rate for the unperturbed system ($A=0$), i.e.,

$$r_0=\frac{1}{\sqrt{2\pi}}\exp\left[-\frac{1}{4D}\right]\ .\tag{6b}$$

Denoting the probability of the system being in the right [left] well by $P^+(t)$ [$P^-(t)$], we propose the rate equations

$$\dot{P}^{\pm}(t)=-r^{\mp}(\omega_0 t+\phi^{\pm})P^{\pm}(t)\tag{7}$$

by assuming local exponential decay with the time-dependent rates $r^{\pm}$ and neglecting recrossing events (i.e., we assume that each trajectory crossing $x=x_u$ is absorbed). The decay processes of P^+ and P^- are considered as two distinct, noninteracting experiments. The phases ϕ^- and ϕ^+ are typically different in our experiments. With $P^{\pm}(t=0)=1$, the solutions of Eq. (7) read

$$P^{\pm}(t)=\exp\left[-\frac{1}{\omega_0}\int_0^{\omega_0 t}r^{\mp}(\theta+\phi^{\pm})d\theta\right]\ .\tag{8}$$

The probability densities for the escape times are thus given by

$$\rho^{\pm}(t)=-\dot{P}^{\pm}(t)$$
$$=r^{\mp}(\omega_0 t+\phi^{\pm})\exp\left[-\frac{1}{\omega_0}\int_0^{\omega_0 t} r^{\mp}(\theta+\phi^{\pm})d\theta\right] . \tag{9}$$

This result is for the escape-time distribution for fixed phases $\phi^{\pm}$. In our analog simulations, however, the phases are not constants, but vary from measurement to measurement.

In the simulation, an escape-time measurement starts immediately *after* a transition from one well to the other and ends when that trajectory leaves the well, as shown in Fig. 1. In the following, we call this interval a "counting interval." The next measurement starts when the trajectory (which is meanwhile not interrupted) arrives again in the *same* well. We thus obtain separate escape-time measurements for both wells. Performing the escape-time statistics, we shift all counting intervals *within one trajectory* to the initial time $t=0$, i.e., we always start with a measurement at $t=0$ but with a randomly different potential configuration described by the phase ϕ. Hence the phase of the modulation, $\theta=\omega_0 t+\phi$, is correlated with the jump of the trajectory from one well to the other,[29] and the phase ϕ, being determined by $\phi=\theta(t=0)$, is also correlated with the jump event. The phase distribution $W^{\pm}(\phi)$ immediately after the jump from the left to the right (+) and from right to left (−) can be obtained within the adiabatic approach by assuming that the jump occurs instantaneously. The jump probabilities from the left to the right (+) and from the right to the left (−) are given as a function of the phase ϕ for small A by

$$P^{\pm}_{\text{jump}}(\phi)=\frac{P_{\text{ad}}(x_u(\phi))}{P_{\text{ad}}(x_s^{\pm}(\phi))}$$
$$\cong N\exp\left[\pm\frac{A}{D}\sin(\phi)\right]+O\left[\frac{A^2}{D},A^2\right] , \tag{10}$$

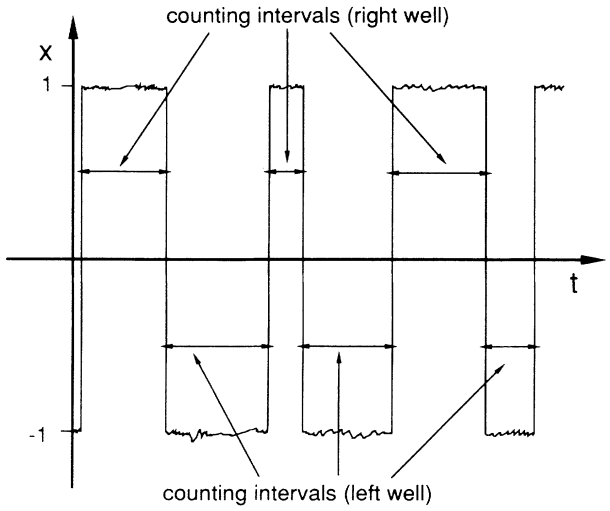

FIG. 1. A stochastic trajectory jumping a few times between left and right wells. The counting intervals are depicted by the double arrows.

where N is a normalization constant. Since we assume that the jump occurs instantaneously, $P^{\pm}(\phi)$ is identical with the probability distribution of the phase after the jump, i.e.,

$$W^{\pm}(\phi)=\frac{1}{2\pi I_0(A/D)}\exp\left[\pm\frac{A}{D}\sin(\phi)\right] , \tag{11}$$

where $I_0(x)$ is the zeroth modified Bessel function. In Fig. 2 the phase distribution functions, Eq. (11), are shown for $A=0.2$ for decreasing values of the noise strength D. For small D, the probability W^{+} becomes very peaked at $\phi=\pi/2$, whereas W^{-} has a peak at $\phi=3\pi/2$. Taking these values as deterministic values for the phase, we obtain from Eqs. (6a) and (9) that the escape-time distributions $\rho^{+}(t)$ and $\rho^{-}(t)$ are identical, as one would expect from the symmetry of the potential.

For finite D the results for the escape-time distributions for fixed phase ϕ must be averaged over the phase distribution functions Eq. (11), i.e.,

$$\langle\rho^{\pm}(t)\rangle_{\phi}=\int_0^{2\pi} W^{\pm}(\phi)r^{\mp}(\omega_0 t+\phi)$$
$$\times\exp\left[-\frac{1}{\omega_0}\int_0^{\omega_0 t} r^{\mp}(\theta+\phi)d\theta\right]d\phi . \tag{12}$$

In general, the integrals in Eq. (12) must be performed numerically. Since $W^{+}(\phi+\pi)=W^{-}(\phi)$ and $r^{+}(\phi+\pi)=r^{-}(\phi)$, the escape-time distributions for both wells are identical, i.e., $\langle\rho^{+}(t)\rangle_{\phi}=\langle\rho^{-}(t)\rangle_{\phi}$. In Fig. 3 the averaged escape-time distribution is plotted for $A=0.2$ and for D ranging from 0.02 to 0.05. The time scale in Fig. 3 is the original, unscaled time scale in milliseconds, and the modulation frequency was $\nu=50$ Hz in the original scaling which results in the dimensionless, scaled frequency $\bar{\omega}_0=2\pi\nu\tau_i=0.0314$. (See Sec. IV.) The

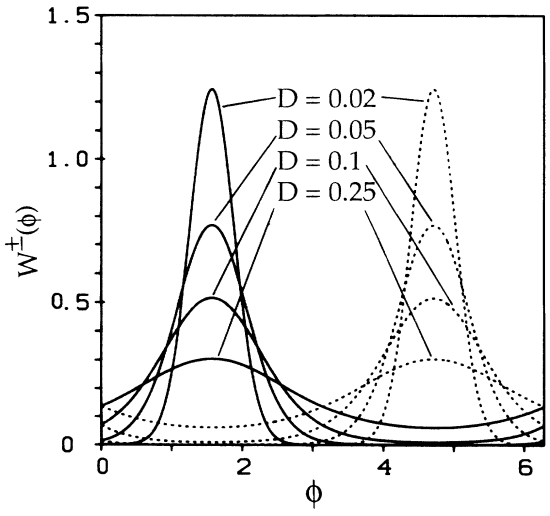

FIG. 2. The phase distributions $W^{+}(\phi)$ (solid lines) and $W^{-}(\phi)$ (dotted lines) are shown for $A=0.2$ V and various values of the noise strength D at the frequency $\nu=50$ Hz ($\omega_0=0.0314$).

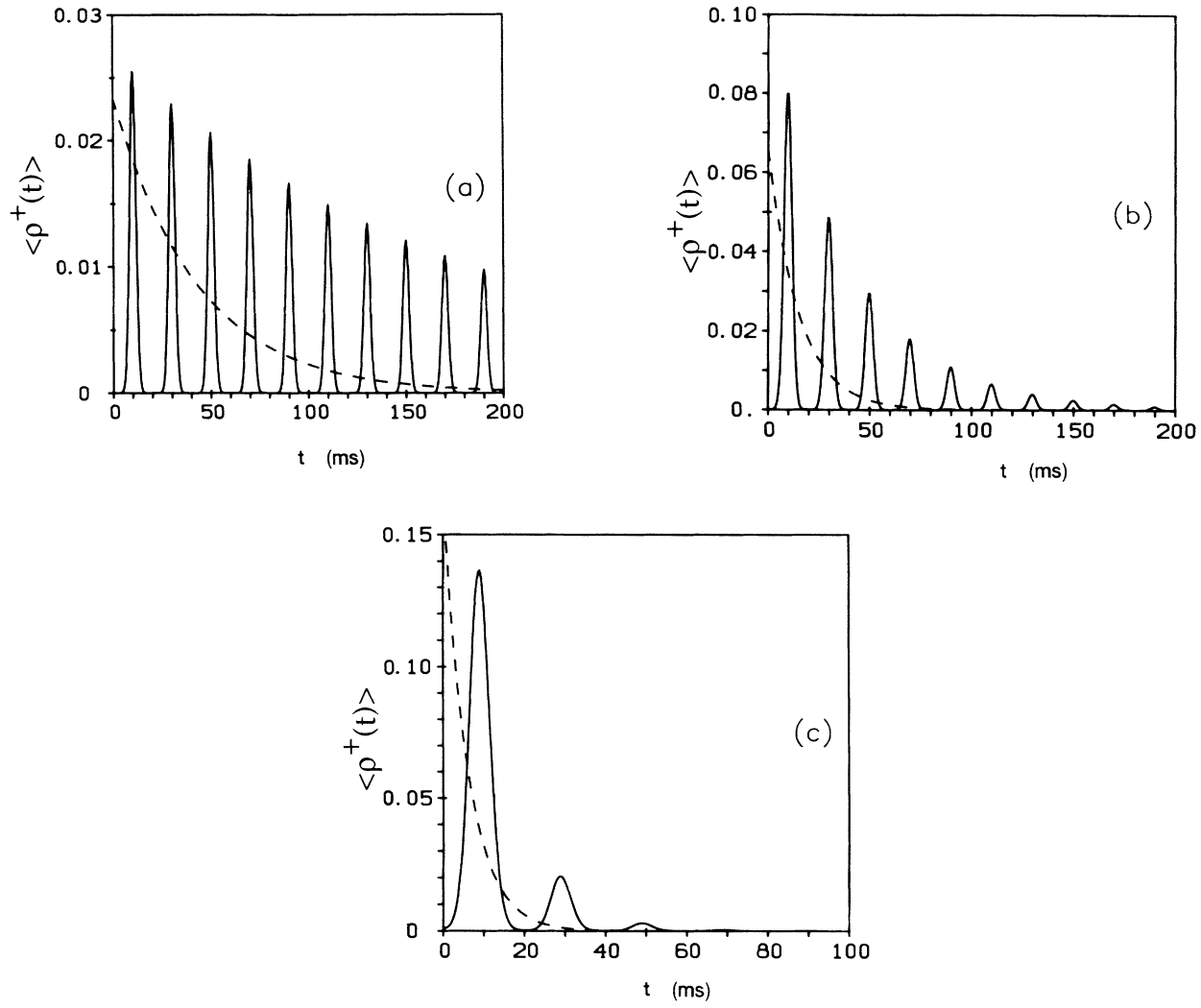

FIG. 3. The escape-time distributions from Eq. (12) are shown for $A=0.2$ V and for (a) $D=0.02$; (b) $D=0.03$; and (c) $D=0.05$ by the solid lines. The dashed lines represent the averaged decay calculated from Eq. (30).

experimentally observed peaks, located at odd multiples of the half period of the modulation frequency as demonstrated in Refs. 18(a) and 19(b), are reproduced by this theory. For increasing D, the peaks gradually vanish, and a monotonic decay of $\rho(t)$ is observed, whereas for decreasing D the peaks become very high. This behavior agrees qualitatively with the measured results of the analog simulation described in Sec. IV. The quantitative agreement is not very good, since most of the measurements were made for values of both A and D that exceed the limits imposed by the adiabatic theory for the modulation frequency used. This defect could, in principle, be remedied by reducing the modulation frequency to a much lower value; however, the experiment then becomes impracticably long in duration.

The most striking feature of these results is the sequence of peaks at odd integer multiples of the half-period of the modulation frequency. It is tempting to connect these peaks with possible subharmonic resonances of the nonlinear, bistable oscillator. It turns out, however, that the power spectrum of our system does *not* show any discernible subharmonics even after very long averaging, as discussed in Ref. 19(b). In order to further investigate this, we performed the phase averaging of the escape-time density in Eq. (12) with a uniform phase distribution, $W^{\pm}(\phi)=1/2\pi$, with the result that the sequence of peaks was destroyed. The origin of the peaks is, therefore, rooted in the *nonuniform* phase distribution $W^{\pm}(\phi)$ given by Eq. (11). In the context of correlation functions and spectral densities, a nonuniform phase distribution leads also to specific predicted behavior.[9,16]

III. ASYMPTOTIC LIMITS AND THE AVERAGED DECAY

A. The limit $A/D \to \infty$

Most of the analog simulations have been performed for small modulation strength and very small noise strength, or for $A \to 0$ and $A/D \to \infty$. In this section we

derive approximate expressions for the escape-time distributions and the peak ratios of the escape-time distributions in this limit. Since the escape rate distributions in both wells are identical, we restrict ourselves in the following to the right well. The time dependent rate r^- is, for these limits, approximated by

$$r^- \cong r_0 \exp\left[-\frac{A}{D}\sin(\omega_0 t+\phi)\right] . \tag{13}$$

The probability P^+ of the trajectory still remaining in the right well is then given by

$$P^+(t)=\exp\left[-\frac{r_0}{\omega_0}\int_0^{\omega_0 t}\exp\left[-\frac{A}{D}\sin(\theta+\phi)d\theta\right]\right] . \tag{14}$$

If $\omega_0 t$ is in the interval $[2n\pi,2(n+1)\pi]$, the integration in Eq. (14) can be carried out from $\theta=0$ to $\theta=2\pi n$, so that

$$P^+(t)=\exp\left[-2\pi n\frac{r_0}{\omega_0}I_0(A/D) - \frac{r_0}{\omega_0}\int_0^{\omega_0\bar{t}}\exp\left[-\frac{A}{D}\sin(\theta+\phi)\right]d\theta\right] , \tag{15}$$

with $\omega_0\bar{t}=\mathrm{mod}(\omega_0 t,2\pi)$. Since the function $\exp(-A/D\sin\theta)$ is strongly peaked at $\theta=\frac{3}{2}\pi$ for $A/D\to\infty$, it is approximately given by the Gaussian

$$\exp\left[-\frac{A}{D}\sin\theta\right]\cong\exp\left[\frac{A}{D}-\frac{1}{2}\frac{A}{D}(\theta+\phi-3\pi/2)^2\right] . \tag{16}$$

Inserting Eq. (16) into Eq. (15) yields

$$P^+(t)=\exp\left[-\frac{r_0}{\omega_0}\left[\frac{\pi D}{2A}\right]^{1/2}\exp\left[\frac{A}{D}\right]\left\{2n-\mathrm{erf}\left[\left[\frac{A}{2D}\right]^{1/2}(\phi-\tfrac{3}{2}\pi)\right]+\mathrm{erf}\left[\left[\frac{A}{2D}\right]^{1/2}(\omega_0\bar{t}+\phi-\tfrac{3}{2}\pi)\right]\right\}\right] , \tag{17}$$

where $I_0(A/D)$ has been replaced by its asymptotic form $\exp(A/D)(2\pi A/D)^{-1/2}$, valid for $A/D\to\infty$, and where $\mathrm{erf}(x)$ is the error function.[27] The phase-dependent escape-time distribution is thus given by

$$\rho^+(t)=\exp\left[-\frac{A}{D}\sin(\omega_0 t+\phi)\right]\exp\left[-\frac{r_0}{\omega_0}\left[\frac{\pi D}{2A}\right]^{1/2}\exp\left[\frac{A}{D}\right]\left\{2n-\mathrm{erf}\left[\left[\frac{A}{2D}\right]^{1/2}(\phi-\tfrac{3}{2}\pi)\right]+\mathrm{erf}\left[\left[\frac{A}{2D}\right]^{1/2}(\omega_0\bar{t}+\phi-\tfrac{3}{2}\pi)\right]\right\}\right] . \tag{18}$$

For $A/D\to\infty$ and $A\to 0$, the phase distribution $W^+(\phi)$ is sharply peaked at $\phi=\pi/2$, so that phase averaging of $\langle\rho^+(t)\rangle$ yields approximately

$$\langle\rho^+(t)\rangle=\exp\left[-\frac{A}{D}\cos(\omega_0 t)\right]\exp\left[-\frac{r_0}{\omega_0}\left[\frac{\pi D}{2A}\right]^{1/2}\exp\left[\frac{A}{D}\right]\left\{2n+1+\mathrm{erf}\left[\left[\frac{A}{2D}\right]^{1/2}(\omega_0\bar{t}-\pi)\right]\right\}\right] . \tag{19}$$

This equation shows peaks approximately at $t_m=(m+\frac{1}{2})T_0$— that is, at odd multiples of the half-period of the driving frequency $\omega_0=2\pi/T_0$— and thus explicitly describes the most striking of the observations made by analog simulation. In Fig. 4 this analytical result (dotted line) is compared to the numerically evaluated escape-time distribution from Eq. (12) (solid line).

The ratio of the heights of any two consecutive peaks is given by

$$\frac{\langle\rho^+(t_{n+1})\rangle}{\langle\rho^+(t_n)\rangle}=\exp\left[-\frac{r_0}{\omega_0}\left[\frac{2\pi D}{A}\right]^{1/2}\exp\left[\frac{A}{D}\right]\right] . \tag{20}$$

valid for $A\to 0$ and $A/D\to\infty$.

B. The limit $A\to 0$ and small A/D

In this limit the escape-time distribution and the peak ratios can be estimated in a similar way to that used

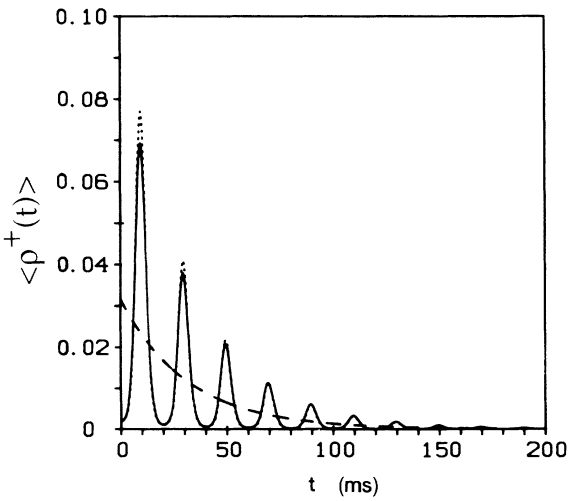

FIG. 4. The numerically evaluated escape-time distribution (solid line) is compared to the analytical result from Eq. (19) (dotted one) and to the averaged decay from Eq. (30) (dashed line) for $A=0.1$ V, $D=0.05$, and $\nu=50$ Hz ($\omega_0=0.0314$).

above for $A/D \to \infty$. Expanding the expression for the time-dependent rate, Eq. (6a) for small A and $A/D \to 0$, we obtain

$$r^-(\omega_0 t+\phi) \cong r_0 \left[1-\frac{A}{D}\sin(\omega_0 t+\phi)+\tfrac{3}{4}A\sin(\omega_0 t+\phi) - \frac{3}{2}\frac{A^2}{D}\sin^2(\omega_0 t+\phi) + \frac{1}{2}\frac{A^2}{D^2}\sin^2(\omega_0 t+\phi) \right] . \quad (21)$$

The probability $P^+(t)$ of the trajectory being still in the right well [having started in the right well with $P^+(0)=1$] is obtained by inserting Eq. (21) into Eq. (8) and neglecting terms of order A^2/D compared to terms of order $(A/D)^2$ and A/D for

$$2n\pi < \omega_0 \bar{t} < (2n+2)\pi ,$$

with the result that

$$P^+(t)=\exp\left[-\frac{n\pi r_0}{\omega_0}\left[2+\frac{A^2}{2D^2}\right] - r_0\bar{t} - \frac{r_0}{\omega_0}\frac{A}{D}[\cos(\omega_0\bar{t}+\phi)-\cos\phi] - \frac{r_0 A^2}{2D^2\omega_0^2}\{\tfrac{1}{2}\omega_0 t - \tfrac{1}{4}\sin[2(\omega_0\bar{t}+\phi)] + \tfrac{1}{4}\sin(2\phi)\} \right] . \quad (22)$$

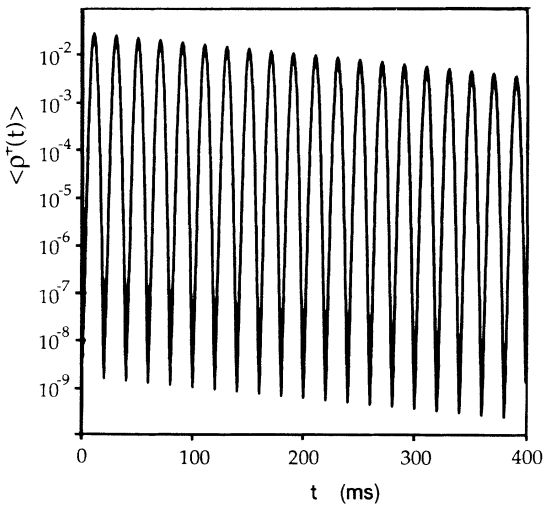

FIG. 5. The numerically evaluated escape-time distribution for $A=0.2$ V, $D=0.013$, and $\nu=50$ Hz ($\omega_0=0.03141$) is shown on a logarithmic scale. The peak-to-peak decrement from these numerical results is 0.902 which can be compared to the prediction of Eq. (20) of 0.906.

Now the escape-time distribution $\rho^+(t)$ can be obtained from Eqs. (22) and (9) and must be averaged over the phase distribution $W^+(\phi)$, which, for $A/D \to 0$, reads

$$W^+(\phi)=\frac{1}{2\pi}\left[1+A/D\sin\phi+A^2/(2D^2)\sin^2\phi-\frac{1}{4}\frac{A^2}{D^2}\right] . \quad (23)$$

After some algebra, we obtain

$$\langle \rho^+(t)\rangle \cong \left[1+\frac{1}{2}\frac{r_0^2}{\omega_0^2}\frac{A^2}{D^2}[1-\cos(\omega_0 t)]\right] r_0\exp(-r_0 t) \quad (24)$$

to leading order in A/D. Note that in this approximation the exponential decay is modulated periodically in time by the time-dependent prefactor.

C. The averaged decay of the escape-time distribution

Let us now discuss the averaged decay of the escape-time distribution—that is, a nonoscillatory smooth curve through the peaked distribution. In Fig. 5, $\langle \rho^+(t)\rangle$ is shown for $D=0.02$ and $A=0.2$ plotted on a logarithmic scale. The envelope of the successive maxima is clearly a straight line, indicating an exponential decay of the maximum amplitudes.[19(b)] The averaged decay can then be expected to also be exponential. We now derive an approximate expression for the decay based on the adiabatic description given above. Assuming uniformly distributed phases, the phase-averaged escape rates for the symmetric potential,

$$\langle r\rangle \equiv \langle r^+\rangle \equiv \langle r^-\rangle = \frac{1}{2\pi}\int_0^{2\pi} r^{\mp}(\omega_0 t+\phi)d\phi , \quad (25)$$

can be evaluated approximately in both limiting cases $A/D \to 0$ and $A/D \to \infty$. The former limit is obtained by inserting Eq. (6a) into Eq. (25), expanding the exponential terms up to order A^2/D and performing the integration, which gives

$$\langle r\rangle = r_0(1+\kappa A^2) , \quad (26a)$$

where

$$\kappa = \frac{1}{4D^2}-\frac{3}{4D} . \quad (26b)$$

Solving the rate equation, Eq. (7), with this averaged escape rate, we find for the averaged escape-time distribution

$$\rho^+(t) \equiv \rho^{\mp}(t) = r_0(1+\kappa A^2)\exp[-r_0(1+\kappa A^2)t] . \quad (27)$$

In the other limit, $A/D \to \infty$, we neglect terms of order A^2/D, A^2, and also terms of order A in the prefactor of Eq. (6a) and insert the results into Eq. (25). For the uniformly averaged rate, we thus obtain

$$\langle r\rangle = r_0 I_0(A/D) , \quad (28)$$

which has the asymptotic form for $A/D \to \infty$,

$$\langle r \rangle \cong r_0 \exp(A/D) \frac{1}{\sqrt{2\pi A/D}} . \quad (29)$$

For the corresponding averaged escape-time distribution, we find

$$\bar{\rho}(t) = r_0 \exp(A/D) \frac{1}{\sqrt{2\pi A/D}} \times \exp\left[-r_0 \exp\left[\frac{A}{D} \right] \frac{t}{\sqrt{2\pi A/D}} \right] . \quad (30)$$

This result is compared to the numerical solutions of Eq. (12) and with the analytical result from Eq. (19) in Figs. 3 and 4, as shown by the broken curves. Equation (30), in fact, gives a quite reasonable approach for the averaged decay. The agreement for $A = 0.2$ V is worse than for $A = 0.1$ V since we have neglected terms of order A^2/D compared with those of order A/D.

D. Peak heights within the adiabatic approximation

The escape-time distribution in the adiabatic limit is given by Eq. (12), and this is the starting point for the numerical computation of the escape-time distribution and its peak heights. The phase distribution $W^{\pm}(\phi)$ given by Eq. (11) is assumed to be sharply peaked at $\phi = \pi/2$, and we therefore replace it with a δ function which leads to Eq. (9) with $\phi = \pi/2$. In order to avoid the $A/D \to \infty, 0$ approximations, the integral in the exponent of Eq. (9) is evaluated numerically. Figure 6 shows the peak heights of the second, third, and fourth peaks as a function of noise strength for $\nu = 500$ Hz and $A = 0.40$ V. The normalization in Fig. 6 was arbitrarily chosen so that the maximum of the second peak is numerically equal to that measured in the analog simulation discussed in Sec. IV. A similar "resonant" phenomenon, called "stochastic resonance," has been extensively studied using the power spectra of $x(t)$ to obtain the signal-to-noise ratios which show a similar maximum with noise strength.[10,13,14,17–19] There is, however, a significant difference between the characterizations based on the power spectra and those based on the escape-time probability densities. In the former case, the full dynamics $x(t)$ from Eq. (1) leads to signal-to-noise ratios which tend to infinity as D tends to zero. This is well understood[14,19] and results from the contributions of interwell motion to the power spectrum when the switching rate becomes much smaller than the experimental observing time, i.e., in the small D limit. This behavior is eliminated in the "two state" model[14] in the theory by considering only the switching events marked by the zero crossings as contributors to the dynamics and in analog simulations by a two state filter.[19] By contrast, in the model and all the simulations considered in this work, the full dynamics is considered, and, as Fig. 6 shows, the peak heights tend to zero with noise strength at least for all peaks of higher order than the first. The peak height of the first peak (not shown in Fig. 6) does not, however, show the familiar resonance behavior. It does tend to zero for large D, but diverges for D tending to zero (as do the nonfiltered signal-to-noise ratio results). This divergence is necessary in order to preserve finite normalization of the probability density. In Sec. IV we show the results of the analog simulations.

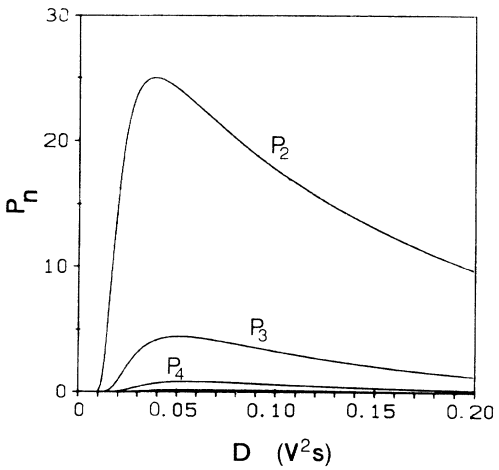

FIG. 6. Numerically evaluated peak heights from Eq. (9) vs noise strength for the second, third, and fourth peaks. The normalization was chosen to agree numerically with the measured data shown in Fig. 9.

IV. ANALOG SIMULATIONS

Following the techniques reviewed previously,[26] we have constructed an analog simulator of Eq. (1) which was driven by quasi-white-noise.[25] The modulation voltage, $A \sin(\omega_0 t)$, was supplied by a Comstron synthesizer having a frequency stability to a few parts in 10^8 per day. The modulation frequencies were either 50 or 500 Hz. The actual noise correlation time was 10 μs and the integrator time constant τ was 0.1 ms. The simulator was operated over a bandwidth of 0 to 100 kHz, and the output voltages were digitized at a 50-kHz rate ($\tau_d = 0.02$ ms per sample) corresponding to a Nyquist frequency of 25 kHz. This can be compared to the quasi-white-noise bandwidth of 0 to 16 kHz (corresponding to the 10-μs correlation time). For the data herein presented, A was either 0.2 or 0.4 V, and D ranged from a low value of 0.02 to a high of 0.05 V^2 s. Unfortunately, these values do not very well represent either of the asymptotic limits presented in Sec. III. The time scales were, however, satisfactory, i.e., $\nu \ll \tau^{-1}$ and $\tau_d \ll \tau \ll \tau_i$.

The noisy voltages from the simulator were digitized in typical 4000-point time series, which were then passed to a PC-AT computer for analysis and ensemble averaging. Typically, 10 000 such time series were analyzed for the zero crossing times, as discussed in Sec. II and shown schematically in Fig. 1, in order to produce one escape-time probability density, as introduced in Ref. 19(b).

Representative examples of our data are shown on Fig. 7, where we present densities $\langle \rho^+(t) \rangle$ measured for the same parameter values as were used in the numerical results shown in Fig. 3. The "signature" of stochastic resonance, peaks in $\langle \rho(t) \rangle$ located at odd multiples of the modulation half-period ($T_0/2 = 10$ ms, $\nu = 50$ Hz), are

clearly revealed. The main discrepancy is that the amplitudes of the peaks in the analog data decay faster than those obtained from the theoretical data. This would indicate a systematic underestimate of the noise intensity D for the analog data. We have previously discussed systematic errors in the determination of D, especially near the white-noise end of the time scale.[19]

We have replotted the data of Fig. 7(a) on a logarithmic scale as shown in Fig. 8 in order to reveal the exponential decay of the peak amplitudes. We see qualitative agreement with the predictions of Eq. (20), however, the measured peak-to-peak decrement is larger than the predicted one by about 12.7%, once again indicating an underestimate of D. Nevertheless, we see that all the main features of the theoretical results are qualitatively reproduced.

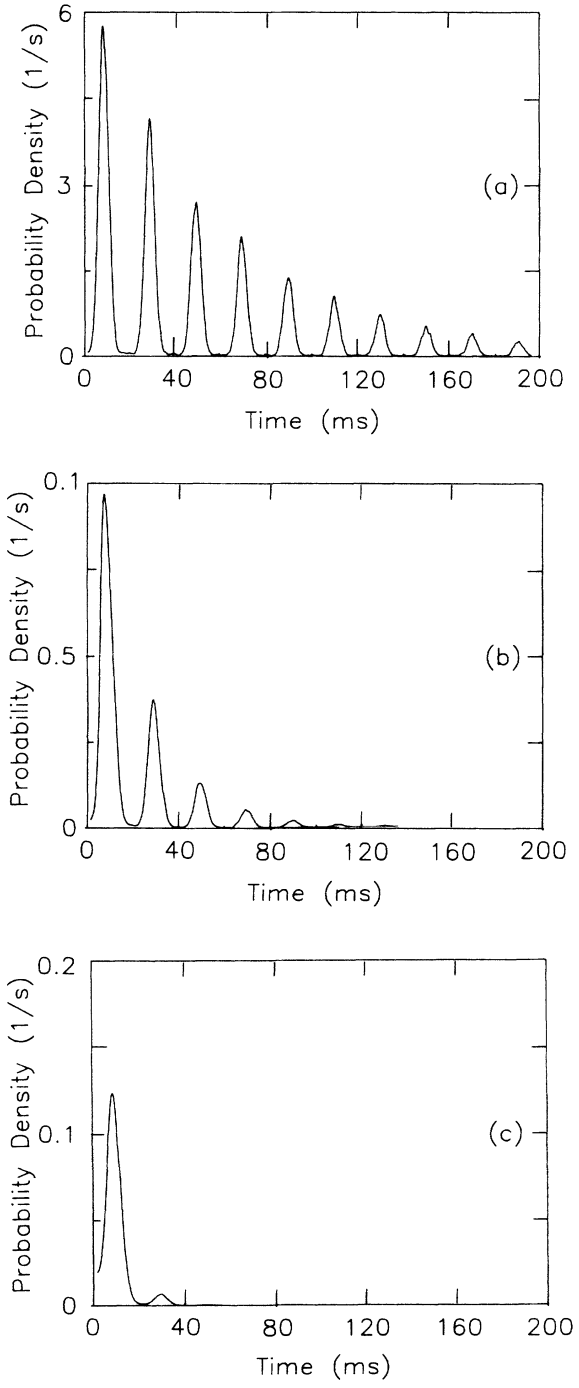

FIG. 7. Measured escape-time probability distributions which can be compared to the numerical results shown in Fig. 3 for the same parameter values: $\nu = 50$ Hz, $A = 0.20$ V, and (a) $D = 0.02$, (b) $D = 0.03$, and (c) $D = 0.05$.

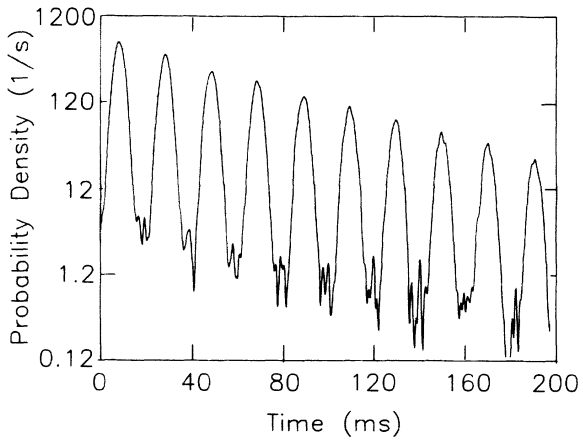

FIG. 8. Same data as Fig. 7(a) replotted on a semilogarithmic scale which reveals the exponential decay of peak amplitudes as also indicated by Eq. (20). The peak-to-peak amplitude decrement measured from the data shown here is 0.719 ± 0.003, which can be compared to the prediction of Eq. (20) which gives 0.628.

In Fig. 9 we plot the peak amplitudes of the second; third- and fourth-order peaks in the escape-time density versus the noise intensity D. These data trace out the familiar stochastic resonance curves which show maxima located at the optimal noise intensities which promote maximum coherent switching rates at those particular multiples of the modulation half-period. The data are qualitatively similar to the curves shown in Fig. 6 where the same quantities were obtained by numerically evaluating the analytic expression Eq. (9). There are two main differences. First, in the analog simulations, we do

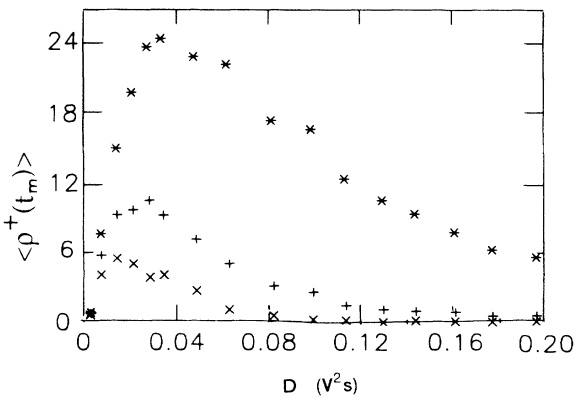

FIG. 9. Measured peak amplitudes of the second (asterisks), third (plus signs), and fourth (crosses) peaks vs noise intensity. Compare with Fig. 6.

not observe the predicted divergence of the first-order peak with D tending to zero for technical reasons. As D becomes small, the switching rate becomes also very small, and a statistically significant sample of escape times (the times between zero crossings) becomes impossible to obtain in a reasonable (even though long) data acquisition time for a single time series. Second, the analog data show the maxima of the higher-order peaks shifted progressively toward smaller values of D, whereas the analytic results do not show this feature. The shift seems reasonable on physical grounds. The higher-order peaks correspond to higher odd multiples of the fundamental half-period $T_0/2$. Switching at these lower frequencies becomes more probable as D becomes smaller.

V. SUMMARY

In this paper we have studied the probability density of escape times as a physical quantity, alternative to the power spectrum, useful for characterizing noise-driven, bistable systems which are periodically modulated. An analytical theory was developed within the framework of the adiabatic approximation, analog simulations of the dynamics were carried out, and the results compared. All features predicted by the theory were qualitatively reproduced by the simulations except for the predicted divergence of the first-order peak in the limit of small noise intensity. A notable feature is the sequence of peaks in the probability density located at odd multiples of the modulation half-period which individually show the resonance phenomenon, i.e., they pass through maxima at optimum values of the noise intensity.

ACKNOWLEDGMENTS

We are grateful to Peter Hänggi, Fabio Marchesoni, and Leone Fronzoni for valuable discussions and a continuing collaboration. P.J. is pleased to thank Stiftung Volkswagenwerk for financial support. This work was supported in part by the Office of Naval Research, Grant No. N00014-88-K-0084, and by N.A.T.O. Grant No. 0770/85.

[1](a) M. H. Devoret, J. M. Martinis, D. Esteve, and J. Clarke, Phys. Rev. Lett. **53**, 1260 (1984); (b) H. M. Devoret, D. Esteve, J. M. Martinis, A. Cleland, and J. Clarke, Phys. Rev. B **36**, 58 (1987).

[2](a) W. C. Schieve, A. R. Bulsara, and E. W. Jacobs, Phys. Rev. A **37**, 3541 (1988); (b) E. W. Jacobs, A. R. Bulsara, and W. C. Schieve, Physica D **34**, 439 (1989).

[3](a) T. Munakata and T. Kawakatsu, Prog. Theor. Phys. **74**, 262 (1985); (b) T. Munakata, *ibid.* **75**, 747 (1986).

[4]S. Martin and W. Martienssen, Phys. Rev. Lett. **56**, 1522 (1986).

[5](a) M. Guevara, L. Glass, and A. Shrier, Science **214**, 1350 (1980); (b) M. Guevara, A. Shrier, and L. Glass, J. Am. Physiol. Soc. (to be published).

[6](a) W. W. Chow, J. Gea-Banacloche, L. M. Pedrotti, V. E. Sanders, W. Schleich, and M. O. Scully, Rev. Mod. Phys. **57**, 61 (1985); (b) M. O. Scully, Phys. Rev. A **35**, 752 (1987); (c) J. Krause and M. O. Scully, *ibid.* **36**, 1771 (1987).

[7](a) M. James and F. Moss, J. Opt. Soc. Am. B **5**, 1121 (1988); (b) J. Y. Gao and L. M. Narducci, Opt. Commun. **58**, 360 (1986).

[8]A. R. Bulsara, W. C. Schieve, and E. W. Jacobs, Phys. Rev. A **41**, 668 (1990).

[9]P. Jung and P. Hanggi, Phys. Rev. A **41**, 2977 (1990).

[10](a) B. McNamara, K. Wiesenfeld, and R. Roy, Phys. Rev. Lett. **60**, 2626 (1988); (b) G. Vermuri and R. Roy, Phys. Rev. A **39**, 4668 (1989).

[11](a) C. Nicolis and G. Nicolis, Tellus **33**, 225 (1981); (b) C. Nicolis, *ibid.* **34**, 1 (1982).

[12](a) R. Benzi, S. Sutera, and A. Vulpiani, J. Phys. A **14**, L453 (1981); (b) R. Benzi, G. Parisi, A. Sutera, and A. Vulpiani, Tellus **34**, 11 (1982).

[13]S. Fauve and F. Heslot, Phys. Lett. **97A**, 5 (1983).

[14]B. McNamara and K. Wiesenfeld, Phys. Rev. A **39**, 4854 (1989).

[15]R. F. Fox, Phys. Rev. A **39**, 4148 (1989).

[16](a) P. Jung, Z. Phys. B **76**, 521 (1989); (b) P. Jung and P. Hanggi, Europhys. Lett. **8**, 505 (1989).

[17]C. Presilla, F. Marchesoni, and L. Gammaitoni, Phys. Rev. A **40**, 2105 (1989).

[18](a) L. Gammaitoni, F. Marchesoni, E. Menichella-Saetta, and S. Santucci, Phys. Rev. Lett. **62**, 349 (1989); (b) L. Gammaitoni, E. Menichella-Saetta, S. Santucci, F. Marchesoni, and C. Presilla, Phys. Rev. A **40**, 2114 (1989).

[19](a) G. Debnath, T. Zhou, and F. Moss, Phys. Rev. A **39**, 4323 (1989); (b) T. Zhou and F. Moss, *ibid.* **41**, 4255 (1990).

[20]M. I. Dykman and M. A. Krivoglaz, Physica **104A**, 480 (1980); **104A**, 495 (1980).

[21]M. I. Dykman, R. Mannella, P. V. E. McClintock, F. Moss, and S. M. Soskin, Phys. Rev. A **37**, 1303 (1988).

[22](a) L. E. Reichl, J. Stat. Phys. **53**, 41 (1988); (b) L. E. Reichl, Z.-Y. Chen, and M. M. Millonas, Phys. Rev. Lett. **63**, 2013 (1989); (c) L. E. Reichl, Z.-Y. Chen, and M. M. Millonas, Phys. Rev. A **41**, 1874 (1990).

[23]J. E. Fletcher, S. Havlin, and G. W. Weiss, J. Stat. Phys. **51**, 215 (1988).

[24]M. James, F. Moss, P. Hanggi, and C. Van den Broeck, Phys. Rev. A **38**, 4690 (1988).

[25]In the simulations described later, we are dealing with real noise having a nonzero correlation time τ. However, we wish to compare our results to a white-noise theory. In the simulations we therefore keep the ratio $\tau/\tau_i = 0.1$, which is a reasonable approximation to white noise within the limits of accuracy of the analog simulator. The integrator time constant τ_i is the system characteristic time by which all other times are scaled. See Ref. 26 for further details.

[26]P. V. E. McClintock and F. Moss, in *Noise in Nonlinear Dynamical Systems,* edited by F. Moss and P. V. E. McClintock (Cambridge University Press, Cambridge, England, 1989), Vol. 3, p. 243.

[27]*Handbook of Mathematical Functions,* edited by M. Abramowitz and I. A. Stegun (Dover, New York, 1965).

[28]In Refs. 19(b) and 23, the inverse of this quantity was called the "residence time;" however, the terms "escape time" and "escape rate" are more familiar when associated to Kramer's formula, and so we will use the latter in the remainder of this paper.

[29]L. Fronzoni and P. Jung (unpublished).